Alzheimer's disease-associated protective variant Plcg2-P522R modulates peripheral macrophage function in a sex-dimorphic manner

Hannah A. Staley[1,2,3], Janna Jernigan[1,2,3], MacKenzie L. Bolen[1,2,3], Ann M. Titus[1,2,3], Noelle Neighbarger[1,2,3], Cassandra Cole[1,2,3], Kelly B. Menees[1,2,3], Rebecca L. Wallings[1,2,3], Malú Gámez Tansey[1,2,3,4*]

[1] Department of Neuroscience, University of Florida College of Medicine, Gainesville, Florida, USA
[2]Center for Translational Research in Neurodegenerative Disease, University of Florida College of Medicine, Gainesville, Florida, USA
[3]McKnight Brain Institute, University of Florida, Gainesville, Florida, USA
[4]Norman Fixel Institute for Neurological Diseases, University of Florida Health, Gainesville, Florida, USA

*Corresponding Author
Malú Gámez Tansey, PhD
mgtansey@UFL.edu

ABSTRACT

Genome-wide association studies have identified a protective mutation in the phospholipase C gamma 2 (*PLCG2*) gene which confers protection against Alzheimer's disease (AD)-associated cognitive decline. Therefore, PLCG2, which is primarily expressed in immune cells, has become a target of interest for potential therapeutic intervention. The protective allele, known as *P522R*, has been shown to be hyper-morphic in microglia, increasing phagocytosis of amyloid-beta (Aβ), and increasing the release of inflammatory cytokines. However, the effect of this protective mutation on peripheral tissue-resident macrophages, and the extent to which sex modifies this effect, has yet to be assessed. Herein, we show that peripheral macrophages carrying the *P522R* mutation do indeed show functional differences compared to their wild-type (WT) counterparts, however, these alterations occur in a sex-dependent manner. In macrophages from females, the *P522R* mutation increases lysosomal protease activity, cytokine secretion, and gene expression associated with cytokine secretion and apoptosis. In contrast, in macrophages from males, the mutation causes decreased phagocytosis and lysosomal protease activity, modest increases in cytokine secretion, and induction of gene expression associated with negative regulation of the immune response. Taken together, these results suggest that the mutation may be conferring different effects dependent on sex and cell type, and highlight the importance of considering sex as a biological variable when assessing the effects of genetic variants and implications for potential immune system-targeted therapies.

Keywords: Alzheimer's disease, macrophage, PLCG2, sex differences

42 **BACKGROUND**

43 Alzheimer's disease (AD) is a devastating neurodegenerative disorder that afflicts millions of
44 people worldwide over two-thirds of which are women (1). Classically, AD is histologically
45 characterized by the presence of amyloid-beta (Aβ) plaques extracellularly, and the formation of
46 tau tangles within neurons. However, over recent years, the immune system has been implicated
47 in the pathogenesis and progression of the disease. Of particular interest are cells of the innate
48 immune system, which includes both peripheral monocytes and macrophages, and the brain-
49 resident macrophages, microglia. These cells are considered to be the body's first line of defense,
50 and are main propagators of inflammation, which has been shown to exacerbate
51 neurodegeneration (2-4). Furthermore, these cells, having the ability to phagocytose, can take up
52 these proteinaceous Aβ plaques as well as dying neurons. It has been noted for some time that
53 although they possess the ability to do so, microglia and peripheral monocytes and macrophages
54 fail to effectively clear these plaques. This has been hypothesized to occur with declining
55 immune function with age, because as the disease progresses, the cells of the immune system
56 become dysregulated, senescent, and associated with low-grade chronic inflammation (5). The
57 lack of disease-modifying interventions for AD until recently has fueled the search for
58 identification of dysregulated immune pathways as potential new targets to delay, arrest, and
59 perhaps prevent disease development (6).

60 Genome-wide association studies identified a mutation within the phospholipase C
61 gamma 2 (*PLCG2*) gene, called *P522R*, that protects against AD-related cognitive decline (7, 8).
62 PLCG2 is highly expressed in immune cells including brain-resident microglia, peripheral
63 monocytes, and tissue-resident macrophages (9). Determining how this mutation confers its
64 protection in these cell populations will allow us to better understand how these cells play a role

65 in the progression of AD, and may open up new avenues for therapeutic development. PLCG2
66 has been shown to support numerous myeloid cell functions including phagocytosis, cytokine
67 secretion, survival, and lipid metabolism (10). To do so, it acts downstream of receptors such as
68 triggering receptor expressed on myeloid cells 2 (TREM2) and toll-like receptors (TLRs) to
69 cleave phosphatidylinositol (4,5) bisphosphate (PIP2) into diacylglycerol (DAG) and inositol
70 1,4,5 triphosphate (IP3). DAG and IP3 go on to both release intracellular calcium and activate
71 downstream pathways including nuclear factor light chain enhancer of activated B cells (NF-κB)
72 (10, 11). The *P522R* mutation has been shown to be hypermorphic, indicating an enhancement of
73 immune cell functions (12). As the primary brain cells that express PLCG2 are microglia, much
74 of the work aimed at investigating how its protective effect is conferred has focused on how it
75 alters microglial function. Studies have shown that the *P522R* mutation increases the release of
76 inflammatory cytokines by microglia, and has variable effects on phagocytosis depending on
77 cargo size (13). For example, studies showed that the *P522R* mutation reduced phagocytosis of
78 *Escherichia coli* but increased phagocytosis of Aβ (14, 15). Further *in vivo* work confirmed this
79 increased uptake of Aβ in a 5XFAD mouse model of amyloid-pathology (16).
80 However, the effect of this mutation in peripheral tissue-resident macrophages has yet to
81 be studied. As this protective pathway is of interest in the development of potential therapeutics,
82 it is important then to understand how those therapeutics may affect the immune system globally,
83 and not just within the brain. Furthermore, peripheral macrophages may not just be bystanders in
84 the progression of AD, as it has been shown that they are not only more efficient phagocytes of
85 Aβ than microglia, but they are also capable of traversing the blood-brain barrier during times of
86 injury and disease (17-21). There is further evidence to suggest this traversal of peripheral
87 myeloid cells to the brain may not even be necessary to impact AD progression. Indeed, studies

88 have shown that AD progression and pathology can be directly impacted by peripheral immune
89 cell functions. For example, Aβ efflux out of the brain and into peripheral reservoirs such as the
90 blood and tissues has been shown to occur (22, 23). The clearance of Aβ from these reservoirs
91 was associated with lower cerebral Aβ pathology (24). Furthermore, peripherally derived Aβ has
92 been shown to enter the brain and exacerbate neuropathology, further supporting the importance
93 of peripheral Aβ stores and clearance (25). Therefore, determining the effect of this protective
94 mutation on peripheral macrophage function is of vital importance.

95 Additionally, given that women are at higher risk for the development of AD, we posit
96 that sex-dependent differences in the immune system may be partially responsible for this
97 increased risk. For instance, it has been well established that females are at greater risk for
98 autoimmune conditions due to an overactive and inflammatory immune system (26). Given that
99 activated microglia and infiltrating monocytes are detectable in the early stages of AD (27), basal
100 over-activation of innate immune cells in females could be a potential link to the increased
101 prevalence of AD in women. Further studies have also shown that relative to healthy control
102 females, females with AD possess a higher prevalence of less phagocytic pro-inflammatory
103 macrophages (28). This could lead to lower Aβ uptake, and over-activation of surrounding
104 immune cells. With this in mind, we determined that sex as a biological variable should be
105 investigated in the present study, as sexually-dimorphic differences have been described for both
106 immune function and risk for AD.

107 The aims of our study were two-fold. First, we aimed to study the effect of the *P522R*
108 mutation on a peripheral macrophage population to determine how these cells may be
109 differentially affected by the mutation. To do so, we assessed changes in major macrophage
110 functions including phagocytosis and inflammatory cytokine secretion, as well as the

111 transcriptional changes that underlie these functions. We utilized peritoneal macrophages
112 (pMacs) which can be separated into two main populations, large peritoneal macrophages
113 (LPMs) and small peritoneal macrophages (SPMs). In broad terms, LPMs are known to be
114 resident to the peritoneal cavity, and SPMs are derived from blood-monocytes, which travel to
115 the peritoneal cavity upon infection or other inflammatory events (29). Recent studies have
116 shown that these recruited monocytes can, over time, differentiate into macrophages that closely
117 mimic the resident LPMs (30). This population was selected over bone-marrow derived
118 macrophages as peritoneal macrophages differentiate within the tissue, which allows them to
119 mold to their environment and experience hormonal changes throughout the animal's lifespan
120 (29, 31, 32). Additionally, this population of peripheral macrophages is well characterized,
121 lending to a more informed study that aims to assess tissue-resident macrophages specifically
122 (29, 31, 32). Furthermore, the immune cells of the peritoneum are of great interest in relation to
123 the gut, which has been identified as a peripheral reservoir for Aβ, and as a conduit of peripheral
124 messengers to the brain via the gut-brain-axis (22, 33). Not only that, but immune responses
125 occurring in this region have been shown to directly activate the brain's insular cortex, a region
126 known to be affected during the preclinical stages of AD (34), which can in turn store this
127 immune-related information and alter the peripheral immune response if reactivated, further
128 supporting a direct connection between the brain and peritoneum (35). Second, we aimed to
129 address how sex may influence the effector functions of this population of macrophages, both
130 with and without the *P522R* mutation, as knowing the baseline sex differences in wild-type (WT)
131 mice would more easily allow us to assess additional effects of the *P522R* mutation. We found
132 that the *P522R* mutation does indeed alter pMac function, supporting the idea that this mutation
133 may potentially have protective effects on the organism due to its expression in the periphery and

134 not just in brain-resident immune cells. However, we also found that the effects of this mutation
135 are largely sexually dimorphic, indicating that future studies should utilize both male and female
136 sexes to better inform potential drug development strategies for the clinic.

137 **METHODS**

138 ***Animals***

139 Congenic mice expressing the *P522R* mutation in the *Plcg2* gene were purchased from the
140 Jackson Laboratory (strain #029598) and housed at the University of Florida McKnight Brain
141 Institute vivarium. Mice heterozygous for the *P522R* mutation were produced by breeding
142 heterozygous mice and C57BL/6 control littermates. They were kept at 22°C in 60-70%
143 humidity and on a 12-hour light-dark cycle and fed *ad libitum*. All animal procedures were
144 approved by the University of Florida Institutional Animal Care and Use Committee and were in
145 accordance with the National Institute of Health Guide for the Care and Use of Laboratory
146 Animals (NIH Publications No. 80-23) revised 1996. Both male and female mice were bred and
147 used in these experiments and were 3-5 months old at the time of sacrifice. Mice were sacrificed
148 via cervical dislocation, and all experiments included 5-6 biological replicates.

149 ***pMac isolation and culture***

150 Three days prior to pMac extraction, mice were injected with 1mL of a 3% thioglycolate
151 (Brewer) solution. Thirty minutes prior to thioglycolate injection mice were injected with 50uL
152 of sustained-release Buprenorphine (ZooPharm) to alleviate pain. After three days, the mice were
153 sacrificed via cervical dislocation. The abdomen was sprayed with 70% ethanol and the skin was
154 split along the midline. Once the peritoneal cavity was exposed, a 10mL syringe filled with
155 10mL of cold RPMI (Gibco, 11875119) was injected into the peritoneal cavity using a 27G
156 needle, avoiding blood vessels. Once the 10mL of cold RPMI was injected, another empty 10mL

157 syringe with a 25-gauge needle was used to withdraw and place the peritoneal fluid into a 15mL
158 Falcon collection tube. Any remaining fluid was aspirated via transfer pipette and placed into the
159 collection tube. Once all mice were sacrificed and peritoneal fluid was collected into separate
160 collection tubes, the fluid was passed through a 70uM nylon filter pre-wet with 5mL of cold
161 HBSS-/- (Gibco, 14175103) into a 50mL conical tube. 5mL of cold HBSS-/- was then placed
162 into the collection tube to rinse any remaining cells and passed through the filter as well. The
163 filter was then washed with 5mL of HBSS-/- and the 50mL tube containing the fluid and HBSS-
164 /- were centrifuged at 400*g* for 5 minutes at 4°C to pellet the cells. If any blood cells were
165 present the pellet was resuspended in 1mL of ammonium-chloride-potassium lysis buffer for 1
166 minute and then centrifuged again at 400*g* for 5 minutes at 4°C. Once all cells were pelleted, the
167 supernatant was aspirated and each pellet was resuspended in 3mL of plating media (RPMI, 10%
168 fetal bovine serum, and 1% penicillin/streptomycin). Viable cells were identified and counted
169 using trypan-blue exclusion on an automated cell counter (Countess™). The volume of growth
170 media was adjusted so that cells were plated at a density appropriate for the intended assay
171 (detailed below). Cells were incubated at 37°C, 5% CO_2 for a minimum of 2-hours to allow
172 macrophages to adhere. Wells were washed with sterile DPBS (Gibco, 14190235) to remove any
173 non-adherent cells, and new, pre-warmed growth media was added.

174 ***Flow Cytometry***

175 For flow cytometry analysis, cells were plated at a density of $3x10^5$ cells/well in a 24-well plate
176 and left to incubate overnight. 1 hour prior to collection, DQ-BSA green (Invitrogen, D12050) was
177 added to each well at a concentration of 10ug/mL to measure protein degradation. After 1 hour,
178 the cells were washed 3 times with sterile phosphate buffered saline (PBS) (Gibco, 10010023),
179 detached from the plate via cell scraper, and then transferred to a 96-well v-bottom plate and

180 centrifuged at 300*g* for 5 minutes at 4°C. The cells were then resuspended in 50uL of PBS
181 containing fluorophore-conjugated antibodies for CD11b (1:100, Biolegend, 101216), MHCII
182 (1:100, Biolegend, 107628), and Live/Dead stain (1:2000, Invitrogen, L34965). The cells were
183 then incubated in the dark at 4°C for 20 minutes at which point they were centrifuged again at
184 300*g* for 5 minutes at 4°C. The cells were then washed with sterile PBS, and this process was
185 repeated twice. The cells were then fixed in 50uL per well of 1% paraformaldehyde in PBS for 30
186 minutes in the dark at 4°C. After 30 minutes the cells were centrifuged at 300*g* for 5 minutes at
187 4°C, resuspended in 200uL of FACs buffer (PBS, 0.5 mM EDTA, 0.1% sodium azide), and taken
188 to the Macs quant analyzer (Miltenyi) for flow cytometric analysis. A minimum of 100,000 events
189 were captured per sample and data were analyzed using FlowJo version 10.6.2 software (BD
190 Biosciences). When validating flow cytometry panels and antibodies, fluorescence minus one
191 controls (FMOCs) were used to set gates and isotype controls were used to ensure antibody-
192 specific binding.

193 ***Phagocytosis Assay***

194 For phagocytosis studies, cells were plated at a density of $5x10^4$ cells/well in a 96-well black
195 wall plate (Cellvis, NC1648269) in triplicate. Cells were left to incubate for 6 hours at 37°C in a
196 5% CO_2 humidified cell culture incubator. 2mL of Live Cell imaging solution (Invitrogen,
197 A59688DJ) was added to each vial of pHrodo green *E. coli* bioparticles (Invitrogen, P35366),
198 equating to a final concentration of 1mg/mL, and these solutions were sonicated for 10 minutes.
199 After sonication, the media was removed from the cells in the plate and replaced with 100uL of
200 *E. coli* bioparticle solution, at which point the plate was placed into an onstage incubator
201 connected to an EVOS M7000 microscope to maintain the cells at 37°C and 5% CO_2 humidified
202 atmosphere throughout the duration of the live-cell imaging. GFP images were captured at 20X

203 magnification with 5 images per well every 30 minutes for 15 hours within each well, and the
204 EVOS Celleste (Version 5) software was used to count cells and determine the integrated optical
205 density of GFP fluorescence within each well over time. Brightfield images were used for
206 automated-focus throughout the time course. Treatment conditions were performed in triplicate
207 wells and averaged for analysis.

208 ***Multiplexed Immunoassays***

209 For inflammatory cytokine secretion, isolated pMacs were plated at a density of $1x10^6$ cells/well
210 in a 6-well plate and treated with either vehicle (PBS) or LPS (O111:B4 Sigma, L4391,
211 Lot#0000185317) at a concentration of 10ng/mL. The cells were then placed in a humidified cell
212 culture incubator at 37°C and 5% CO_2. Conditioned media was collected at 2, 6, and 24 hours
213 post stimulation for assessment of specific protein concentrations of TNF, IL-6, IL-1β, KC/GRO,
214 IL-4, IL-10, IFN-γ, IL-5, IL-2, and IL-12p70 (MSD, K15048D-2) using multiplexed
215 immunoassays on the MesoScale Discovery (MSD) platform. Samples were plated in duplicate
216 at a 1:1 dilution with MSD diluent 41 and the rest of the experimental procedure was performed
217 according to the manufacturer's instructions. The plate was then analyzed on the MSD
218 Quickplex machine and MSD software (Discovery Workbench Version 4.0). Cytokines with
219 values below the lower limit of detection (LLOD listed below) were not quantified, these being
220 0.10pg/mL for TNF, 0.04pg/mL for IFN-γ, 0.11pg/mL for IL-1β, 0.22pg/mL for IL-2,
221 0.11pg/mL for IL-4, 0.06pg/mL for IL-5, 0.61pg/mL for IL-6, 0.94 pg/mL for IL-10, 9.95pg/mL
222 for IL-12p70, and 0.24pg/mL for KC/GRO.

223 ***RNA Isolation***

224 For RNA extraction, cells were plated at $1x10^6$ cells/well in a 6-well plate and treated with either
225 vehicle or LPS at 10ng/mL. The cells were placed back in a humidified cell culture incubator at

226 37°C and 5% CO_2 for 6 hours. Buffer RLT from the RNeasy mini kit (Qiagen, 74104) was
227 combined with β-mercaptoethanol (Sigma, 63689) at a concentration of 20uL of BME per 1mL
228 of buffer RLT. Media was aspirated from the plate and then 350uL of RLT+BME solution was
229 then added to each well to lyse the cells. Each well was scraped with a mini cell scraper (Fisher,
230 NC0325221) and collected into a Qiashredder (Qiagen) column and centrifuged at 10,000*g* for 2
231 minutes. 350uL of 70% ethanol was added to the homogenized lysate and then transferred to a
232 RNeasy spin column. The columns were then centrifuged for 30 seconds at 10,000*g* and
233 afterwards the flow-through was discarded. 700uL of buffer RW1 was then added to each
234 column and the columns were centrifuged at 10,000*g* for 30 seconds and the flow-through was
235 discarded. 500ul of buffer RPE was added to each column and they were spun at 10,000*g* for 2
236 minutes and the flow-through was again discarded. This step was repeated twice, and the column
237 was then placed into a 1.5mL collection tube, 30uL of elution buffer was added to the column,
238 and then centrifuged for 1 minute at 10,000*g* to elute the RNA. Concentration of RNA was
239 analyzed on a spectrophotometer, and RNA quality was assessed using Bioanalyzer 2100
240 (Agilent, Denmark).

241 ***Gene expression analysis***

242 For quantification of mRNA transcripts in pMacs, the NanoString nCounter platform and Mouse
243 Immune Exhaustion Panel RNA (CAT#PSTD-M-EXHAUST-12) containing 785 genes was
244 used. 25ng/ul of RNA was loaded and hybridized to the provided capture and reporter probes
245 overnight at 65°C according to the manufacturer's instructions. The samples were then added
246 into the provided nCounter chip via the use of the NanoString MAX/FLEX
247 robot. Unhybridized capture and reporter probes were removed, and the hybridized mRNAs were
248 immobilized for transcript count quantification on the nCounter digital analyzer. The data was

249 then imported into the nSolver analysis software v4.0 for quality check and analysis according to
250 the manufacturer's instructions. Raw counts were normalized to the geometric mean of the
251 positive and negative controls and count expression was calculated via nSolver Advanced
252 Analysis v2.0.134. Gene expression was considered significant if $p < 0.05$ after adjustment using
253 the Benjamini-Hochberg method for false discovery rate, and if the fold change was greater than
254 1.5. Pathway analysis was performed using Enrichr for GO biological process analysis (36-38).

255 ***Statistical Analysis***

256 Statistical analysis was performed using Prism Graphpad version 10.2.2. Differences between
257 groups was determined using either T-test with Welch's correction or 2-way ANOVA with
258 multiple comparisons using Tukey's post-hoc correction. Results were considered statistically
259 significant if $p < 0.05$. Each graph depicts individual data points with error bars representing the
260 standard error of the mean (SEM).

261

262 **RESULTS**

263 ***The P522R mutation does not alter pMac sub-populations in male mice but increases antigen***
264 ***presentation***

265 Before addressing cellular functionality, it is beneficial to first understand and characterize the
266 macrophage populations present within our samples. As mentioned, pMacs are not a
267 homogenous population, with SPMs arising from blood monocytes and LPMs being resident to
268 the peritoneal cavity. To determine whether the *P522R* mutation has any effect on the
269 frequencies of these cell populations we isolated pMacs from the peritoneal cavity of male mice,
270 and then used flow cytometry to distinguish SPMs from LPMs on the basis of CD11b
271 expression, as has been previously described (Supplemental Figure 1A) (39). Prior to isolation,

272 we performed an intraperitoneal injection of a 3% thioglycolate solution. This step is crucial
273 prior to isolation, as it allows us to harvest both LPMs and SPMs, not just the resident LPMs.
274 However, we do allow a three-day rest period post injection and prior to cell isolation so that
275 acute inflammation and cell activation induced by the injection subside (Figure 1).

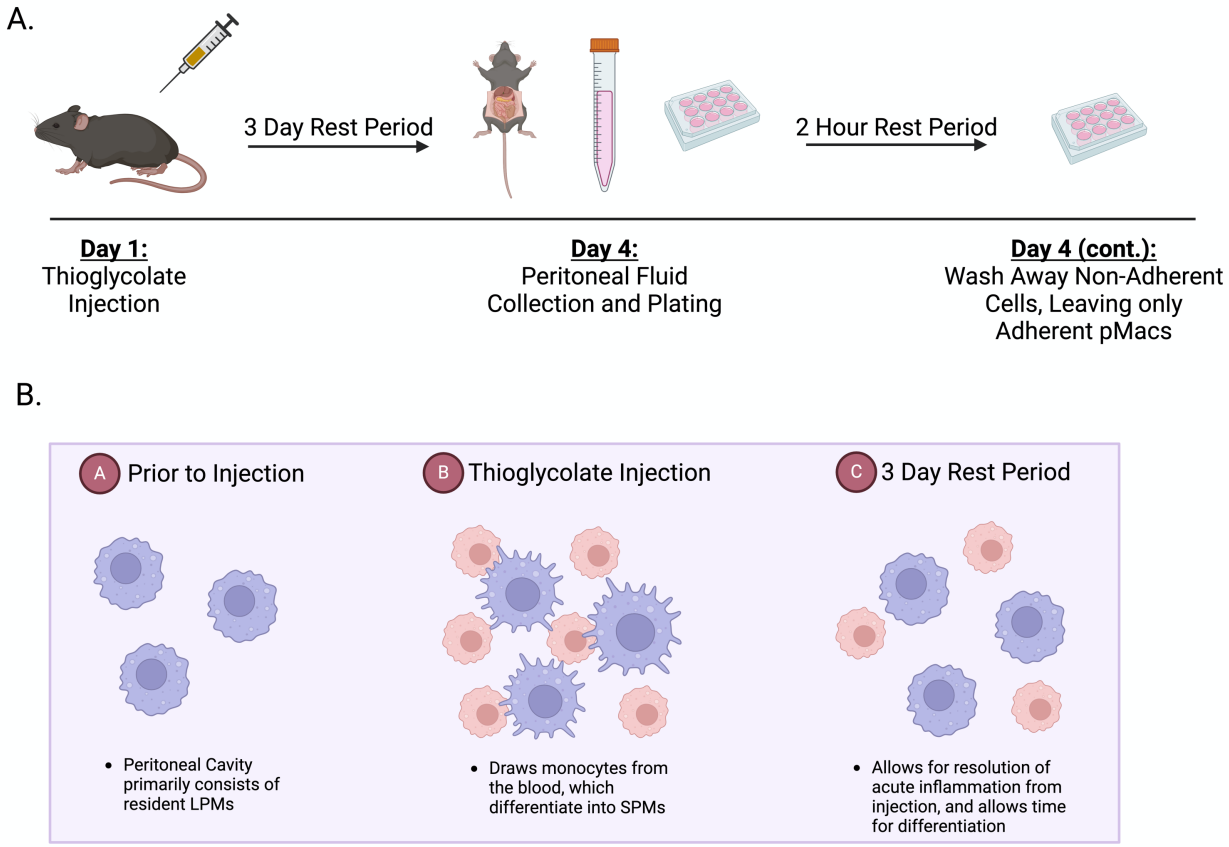

276

277 **Figure 1: Schematic of pMac collection and the purpose of thioglycolate injections prior to cell isolation.**
278 Diagram describing the process of pMac isolation (A) and visual representation of the purpose of starting the
279 process with a thioglycolate injection (B). Created with Biorender.com.
280
281 Additionally, after plating the cells collected from the peritoneum, we leave the cells to rest for
282 two hours and then rinse with sterile DPBS and replace the media, as this allows only the
283 adherent cells (pMacs) to remain and all other immune cell types to be washed away
284 (Supplemental Figure 1B). We further confirmed LPM vs SPM populations by assessing
285 canonical peritoneal macrophage markers of LPMs (CD80 and F4/80) and SPMs (Dectin1)

286 (Supplemental Figure 1C-E). We found that male mice carrying the *P522R* mutation showed no
287 difference in the frequency of either LPM or SPM sub-populations compared to WT male mice
288 (Figure 2A, B). This was confirmed via raw counts (Supplemental Figure 2A-D). Next, we used
289 major histocompatibility complex class II (MHCII) as a marker of antigen presentation. We
290 found that although LPM and SPM populations were not affected by the *P522R* mutation in male
291 mice, antigen presentation on LPMs was. A higher frequency of LPMs were MHCII+ in *P522R*
292 males compared to LPMs from WT males (Figure 2C).

293 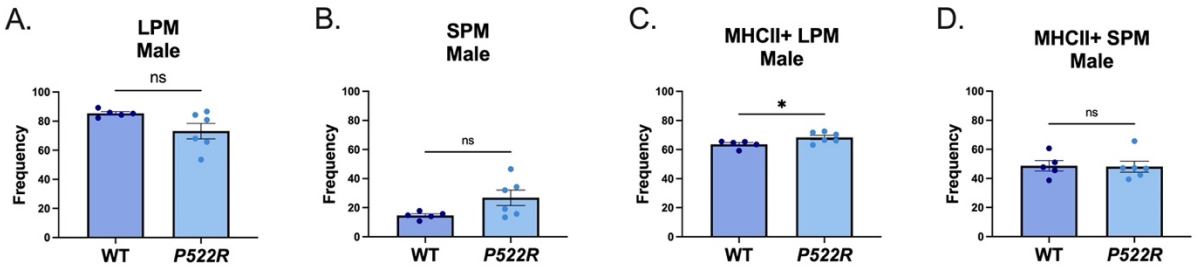

294 **Figure 2: The *P522R* mutation does not alter pMac sub-populations in male mice but increases antigen**
295 **presentation.** To determine the prevalence of different sub-populations of macrophages in our *ex vivo* cultures
296 pMacs from male WT and *P522R* animals were isolated, plated, and non-adherent cells were washed away after a 2-
297 hour rest period and populations of (A) LPM (B) SPM (C) MHCII+ LPM and (D) MHCII+ SPM were quantified via
298 flow cytometry. Data was quantified via T-test with Welch's correction. Groups are considered non-significant if
299 $p>0.05$ and significantly different if $p<0.05$.

300 We did not find any significant differences between *P522R* and WT males in MHCII expression
301 on SPMs (Figure 2D). Representative plots for this analysis can be found in Supplemental Figure
302 2E and 2F. These data indicate that in males the *P522R* mutation does not affect the makeup of
303 peritoneal macrophage sub-populations, but does increase the amount of resident LPMs
304 displaying antigens.

305 ***The P522R mutation alters both sub-populations and antigen presentation in pMacs from***
306 ***female mice***

307 Based on the literature indicating distinct sex-differences in pMac populations, we aimed to
308 determine whether the *P522R* mutation would have similar effects on population frequencies and

309 antigen presentation in female mice as was seen in male mice (40). However, we found that the
310 *P522R* mutation had quite different effects in female mice compared to those seen in male mice.
311 Female mice carrying the *P522R* mutation exhibited significant increases in the frequency of
312 LPMs, and significantly lower frequencies of SPMs compared to WT females (Figure 3A, B).
313 After reviewing the counts, we determined that these effects were primarily driven by an
314 increase in the raw count of LPMs in females that carry the *P522R* mutation (Supplemental
315 Figure 3A-D). Furthermore, contrary to the effect seen in pMacs from males, the *P522R*
316 mutation's presence in females actually decreased the frequency of MHCII+ LPMs compared to
317 pMacs from WT females (Figure 3C). But similar to males, there were no observable differences
318 between the frequencies of MHCII+ SPMs between WT or *P522R* females (Figure 3D),
319 representative plots for which can be found in Supplemental Figure 3E and 3F.

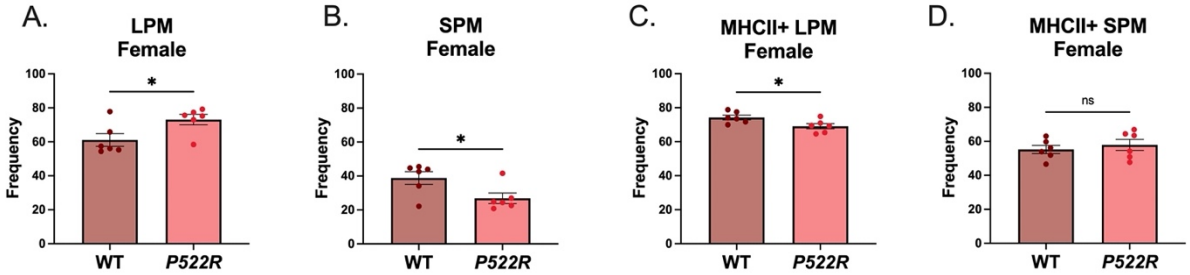

320

321 **Figure 3: The *P522R* mutation alters both sub-populations and antigen presentation in pMacs from female**
322 **mice.** To determine the prevalence of different sub-populations of macrophages in our *ex vivo* cultures pMacs from
323 female WT and *P522R* animals were isolated, plated, and non-adherent cells were washed away after a 2-hour rest
324 period and populations of (A) LPM (B) SPM (C) MHCII+ LPM and (D) MHCII+ SPM were quantified via flow
325 cytometry. Data was quantified via T-test with Welch's correction. Groups are considered non-significant if $p>0.05$
326 and significantly different if $p<0.05$.
327
328 These data support a role for the *P522R* mutation in altering macrophage sub-populations within
329 the peritoneum of female mice. However, these effects are largely sex-specific, and even bi-
330 directional in the case of antigen presentation. These data begin to confirm a role for the *P522R*
331 mutation in peripheral tissue resident macrophages, and further support previously published
332 data indicating significant sex-differences in immune cell populations and function.

333 ***The P522R mutation reduces phagocytic capacity and lysosomal protease activity in pMacs***
334 ***from males***
335 After determining that the *P522R* mutation can alter pMac populations in female mice, and
336 antigen presentation on LPMs in a bidirectional manner in females and males, we aimed to
337 determine whether this mutation also has functional consequences in pMacs from each sex.
338 Macrophages are known to have many dynamic functions, yet phagocytosis and cytokine
339 secretion are among the most recognized, both of which PLCG2 is actively involved in. We
340 began with assessing phagocytosis capabilities in pMacs from male WT and *P522R* mice, as the
341 ability to uptake and degrade bacterial/viral particles is among the most important functions of
342 macrophages in the fight against infection. Furthermore, this function has been directly
343 associated with AD, as *E. coli* particles and LPS particles have been shown to associate directly
344 with pathology in the brains of AD patients (41). Additionally, AD progression has been
345 correlated with infection, emphasizing the importance of the pMacs ability to uptake and degrade
346 bacterial particles (42). To assess the phagocytic capabilities of these macrophages, we utilized
347 fluorescently labeled *E. coli* bioparticles which only fluoresce after being internalized and
348 exposed to the low pH associated with the lysosome, thereby reporting on the extent of bacterial
349 uptake by the cells. Interestingly, we found that pMacs from *P522R* male mice performed less
350 uptake of the fluorescent *E. coli* over the course of 15 hours than did pMacs from WT male mice
351 (Figure 4A-C). Up until approximately the 6 hour mark, the *P522R* and WT pMacs performed
352 very similar amounts of *E. coli* uptake, but the *P522R* pMacs were not able to keep up with the
353 WT pMacs, which seemingly performed better (Figure 4B). Although the macrophages were
354 able to take up the *E. coli* particles, we further assessed whether pMacs from males displayed
355 any differences in lysosomal function, or the ability to successfully break down that which has

356 been phagocytosed. To do so, we treated the cells with DQ-BSA, a substrate for proteases that

357 only fluoresces after it has been cleaved within the lysosome, and quantified via flow cytometry.

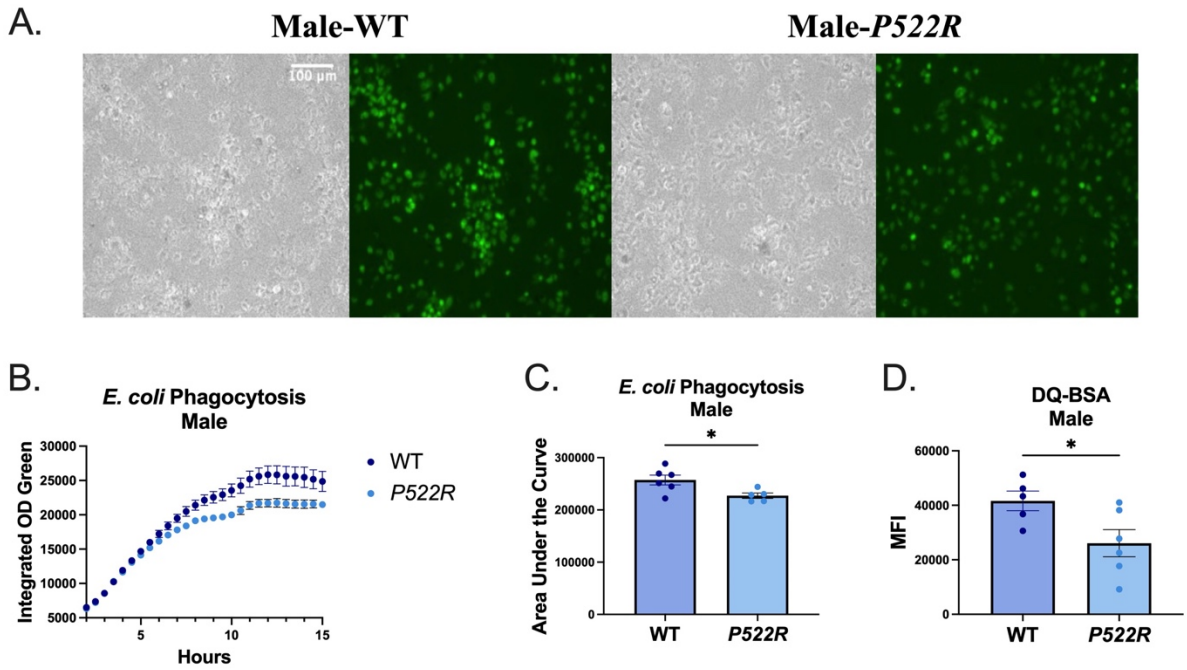

358

359 **Figure 4: The *P522R* mutation reduces phagocytic capacity and lysosomal protease activity in pMacs from**
360 **males.** pMacs from WT and *P522R* males were plated and incubated for 6 hours, at which point 200ug of *E. coli*
361 was added to each experimental well to assess *E. coli* uptake. (A) Representative brightfield images and GFP
362 fluorescence for each group are presented at 20X magnification. (B) Integrated optical density of GFP fluorescence
363 was plotted over 15 hours. (C) Groups were compared statistically via area under the curve. 1 hour prior to cell
364 collection DQ-BSA was added to the plate and then cells were collected for flow cytometry and (D) DQ-BSA MFI
365 is represented. Groups are considered non-significant if $p>0.05$ and significantly different if $p<0.05$.
366

367 Again, we found that pMacs from WT males performed better than pMacs from *P522R* males,

368 which exhibited lower lysosomal protease activity compared to pMacs from WT males (Figure

369 4D). These data indicate that the *P522R* mutation does indeed alter phagocytosis and lysosomal

370 activity in males, but these alterations may not be beneficial to pMac function.

371 ***The P522R mutation does not alter phagocytic capacity in pMacs from females, but increases***

372 ***lysosomal protease activity***

373 As the *P522R* mutation has been associated with protection, the decrease in phagocytic capacity

374 and lysosomal protease activity seen in pMacs from *P522R* males was quite surprising. We

375 repeated both the *E. coli* uptake assay, as well as the DQ-BSA lysosomal protease activity assay
376 in pMacs from WT and *P522R* females to determine whether similar patterns were seen in
377 females. Similar to what we found in our assessment of pMac populations, the *P522R* mutation
378 had different effects in pMacs from females compared to pMacs from males. Although there
379 appeared to be a visual difference in GFP fluorescence between pMacs from *P522R* and WT
380 females, quantification showed that uptake of *E. coli* in pMacs from females was largely
381 unaffected by the *P522R* mutation (Figure 5A-C). However, lysosomal protease activity
382 measured via fluorescence of the DQ-BSA probe was shown to be increased in pMacs from
383 *P522R* females (Figure 5D).

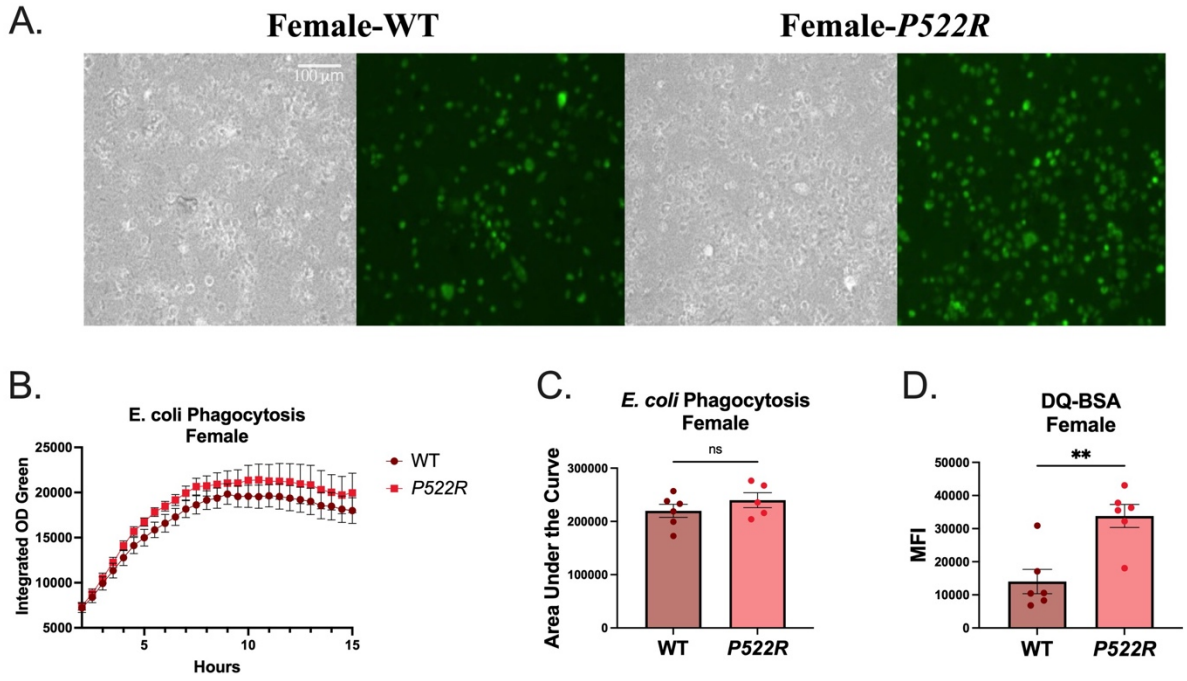

384

385 **Figure 5: The *P522R* mutation does not alter phagocytic capacity in pMacs from females, but increases**
386 **lysosomal protease activity.** pMacs from WT and *P522R* females were plated and incubated for 6 hours, at which
387 point 200ug of *E. coli* was added to each experimental well to assess *E. coli* uptake. (A) Representative brightfield
388 images and GFP fluorescence for each group are presented at 20X magnification. (B) Integrated optical density of
389 GFP fluorescence was plotted over 15 hours. (C) Groups were compared statistically via area under the curve. 1
390 hour prior to cell collection DQ-BSA was added to the plate and then cells were collected for flow cytometry and
391 (D) DQ-BSA MFI is represented. Groups are considered non-significant if $p>0.05$ and significantly different if
392 $p<0.05$.
393

394 These data indicate that the *P522R* mutation may confer functional advantages in lysosomal
395 activity in pMacs from females, but not in males.

396 ***The P522R mutation modestly increases inflammatory cytokine secretion by pMacs from***
397 ***males***

398 As mentioned, the other function of macrophages that has been linked to PLCG2 function is
399 cytokine secretion. We have already demonstrated that the *P522R* mutation has sex-dependent
400 effects on phagocytosis and lysosomal function, and we hypothesized that it would also alter
401 cytokine secretion by pMacs, likely also in a sex-dependent manner. To test this, we treated
402 pMacs from WT and *P522R* males with LPS and measured the protein concentration of
403 cytokines within the media at 2, 6, and 24 hours post-LPS treatment. We found that vehicle
404 treated cells produced very low concentrations of inflammatory cytokines, with no difference
405 between WT and *P522R* cells, further supporting that our *ex vivo* cultures are not activated or
406 inflammatory at baseline conditions (Figure 6A-H). For this reason, we treated with the immune
407 cell stimulant LPS to elicit an inflammatory response, as although there were no genotype
408 differences at baseline, the different genotypes may respond differently to inflammatory stimuli.

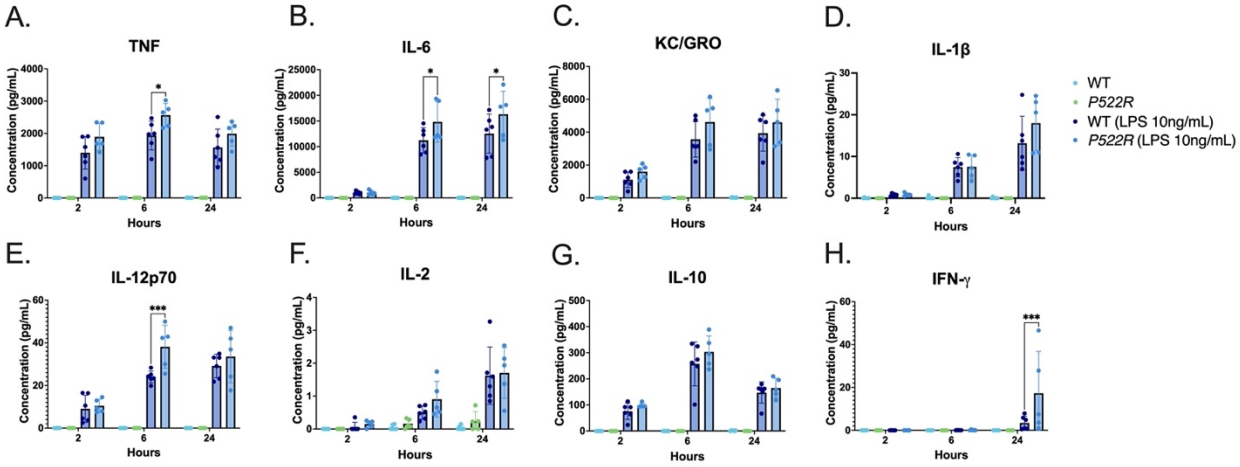

409

410 **Figure 6: The *P522R* mutation modestly increases inflammatory cytokine secretion by pMacs from males.**
411 pMacs from male WT and *P522R* mice were plated and treated with LPS, and their conditioned media was collected
412 at 2, 6, and 24 hours post LPS stimulation. Concentrations of (A) TNF (B) IL-6 (C) KC/GRO (D) IL-1β (E) IL-

12p70 (F) IL-2 (G) IL-10 and (H) IFN-γ were then assessed via MesoScale Discovery immunoassays. Data were quantified via two-way ANOVA using Tukey's post-hoc correction for multiple comparisons. Groups are considered non-significant if $p>0.05$ and significantly different if $p<0.05$.

Indeed, we found that upon LPS stimulation, pMacs from *P522R* males showed modest increases in inflammatory cytokine secretion of TNF, IL-6, and IL-12p70 at 6 hours post-LPS stimulation (Figure 6A, B and E), and IFN-γ at 24 hours post-LPS stimulation compared to pMacs from WT males (Figure 6H). We found no differences between genotypes in secretion of KC/GRO, IL-1β, IL-2, or IL-10 even after LPS stimulation (Figure 6C, D, F and G). These data support that the *P522R* mutation has a modest effect on pMac cytokine secretion in males.

The P522R mutation increases inflammatory cytokine secretion by pMacs from females

To determine whether these same stimulation dependent effects were seen in females, we repeated this same experiment but with pMacs from WT and *P522R* females. Similar to pMacs from males, we found the pMacs from both WT and *P522R* females produce very low levels of inflammatory cytokines when not stimulated with LPS (Figure 7A-H), supporting that, like our male cultures, the female *ex vivo* cultures are not inflammatory or activated prior to stimulation.

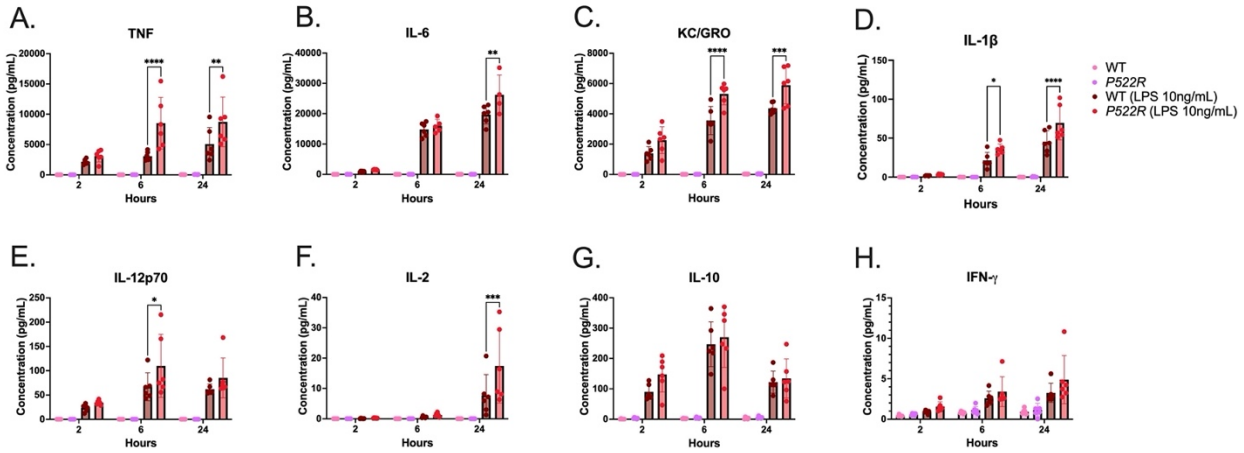

Figure 7: The *P522R* mutation increases inflammatory cytokine secretion by pMacs from females. pMacs from female WT and *P522R* mice were plated and treated with LPS, and their conditioned media was collected at 2, 6, and 24 hours post-LPS stimulation. Concentrations of (A) TNF (B) IL-6 (C) KC/GRO (D) IL-1β (E) IL-12p70 (F) IL-2 (G) IL-10 and (H) IFN-γ were then assessed via MesoScale Discovery immunoassays. Data were quantified via two-way ANOVA using Tukey's post-hoc correction for multiple comparisons. Groups are considered non-significant if $p>0.05$ and significantly different if $p<0.05$.

436 Similar to what we saw in our male data, LPS stimulation did reveal genotype-dependent
437 differences in cytokine secretion, however these differences were different and more prevalent
438 than in our male cultures. For example, at 6 hours post-LPS stimulation, pMacs from *P522R*
439 females were secreting more TNF, KC/GRO, IL-1β, and IL-12p70 than pMacs from WT females
440 (Figure 7A, C, D, and E). At 24 hours post-LPS stimulation, pMacs from *P522R* females were
441 secreting more TNF, IL-6, KC/GRO, IL-1β, and IL-2 compared to pMacs from WT females
442 (Figure 7A-D, and F). We found no genotype dependent differences in IL-10 or IFN-γ at any
443 time point (Figure 7G, H). So, although the *P522R* mutation caused increases in cytokine
444 secretion by pMacs from both males and females, the pMacs from females seemed to be more
445 affected by the presence of the mutation and produced significantly more inflammatory
446 cytokines over time.

447 ***Genes selectively upregulated in P522R males are associated with negative regulation of the***
448 ***immune response***

449 In our selected assays, the *P522R* mutation seemed to have a dampening effect on pMacs from
450 males, indicating a potential sex-specific role for the mutation. Furthermore, many of these
451 differences were more noticeable after treatment with some sort of immune cell stimulant, such
452 as *E. coli* or LPS, supporting the idea that the *P522R* mutation's effects may be activation-
453 dependent, and not as prevalent under baseline conditions. To attempt to identify molecular
454 pathways associated with the effects of stimulation, we performed a targeted transcriptomic
455 analysis using Nanostring nCounter to assess 785 genes associated with immune cell function in
456 pMacs from both WT and *P522R* males. We did so both at baseline and after treatment with LPS
457 to determine whether these effects were truly activation dependent. As expected, we did not find
458 any significant differences in gene expression between pMacs from WT and *P522R* males under

459 baseline conditions (Supplemental Figure 5A). However, after treatment with LPS, differences

460 between the genotypes did begin to arise.

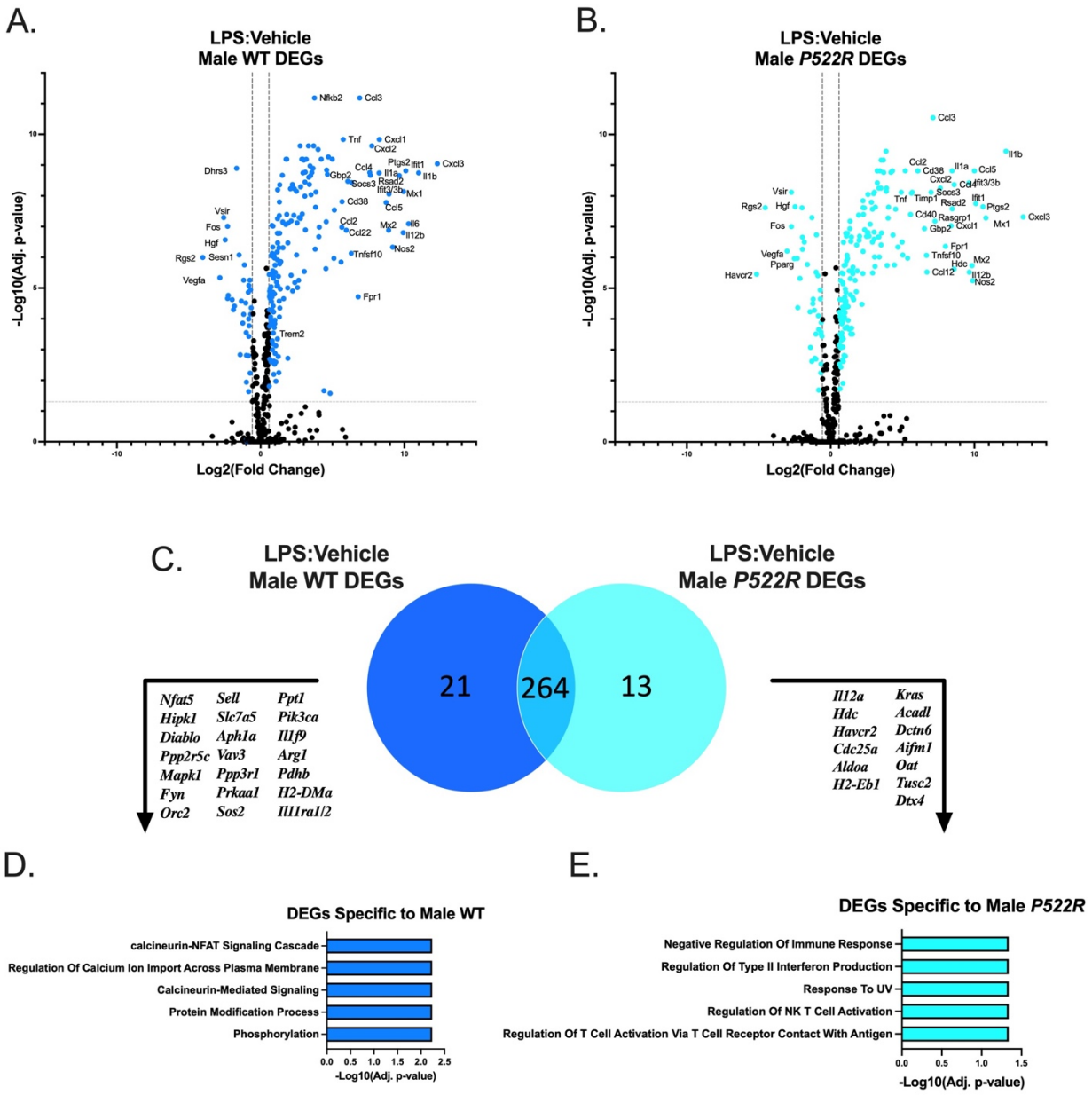

461

462 **Figure 8: Genes selectively upregulated in *P522R* males are associated with negative regulation of the immune**
463 **response.** pMacs from male WT and *P522R* mice were plated and treated with either vehicle or LPS (10ng/mL) and
464 left to incubate for 6 hours. Cells were then collected and RNA was isolated for gene expression analysis. (A)
465 Volcano plot comparing gene expression of LPS treated pMacs from male WT mice to gene expression of vehicle
466 treated pMacs from male WT mice, horizontal grey dashed line indicating adjusted $p<0.05$, and vertical dashed lines
467 indicating fold change of greater than 1.5. (B) Volcano plot comparing gene expression of LPS treated pMacs from
468 male *P522R* mice to gene expression of vehicle treated pMacs from male *P522R* mice, horizontal grey dashed line
469 indicating adjusted $p<0.05$, and vertical dashed lines indicating fold change of greater than 1.5. (C) Venn diagram
470 comparing number of DEGs between pMacs from WT males and pMacs from *P522R* males after LPS stimulation.

471 (D) GO biological process pathways associated with DEGs specific to pMacs from WT males in response to LPS
472 stimulation. (D) GO biological process pathways associated with DEGs specific to pMacs from *P522R* males in
473 response to LPS stimulation.
474
475 Volcano plots representing each genotype's response to LPS stimulation are represented in
476 Figure 8A and 8B, with 8A showing pMacs from WT male's response to LPS, and 8B showing
477 pMacs from *P522R* male's response to LPS. We found that many of the differentially expressed
478 genes (DEGs) induced by LPS stimulation were shared between pMacs from WT and *P522R*
479 males, encompassing 264 shared DEGs (Figure 8C). However, there were a number of genes that
480 were genotype specific, including 13 DEGs specific to *P522R* males, and 21 specific to WT
481 males (Figure 8C). We took each of these sets of genotype specific genes and assessed what
482 pathways were associated with them. We found that the DEGs specific to pMacs from WT males
483 were associated with pathways including calcineurin-NFAT signaling cascade, regulation of
484 calcium ion transport across the plasma membrane, calcineurin-mediated signaling, and protein
485 modification/phosphorylation (Figure 8D). Many of these pathways involve calcium signaling,
486 and the calcineurin cascade which in macrophages has been shown to down-regulate TLR
487 mediated activation pathways (43). Contrarily, the DEGs specific to pMacs from *P522R* males
488 were associated with pathways including negative regulation of immune responses, regulation of
489 type II interferon production, regulation of NK T cell activation, and response to UV (Figure
490 8E). These results suggest that the *P522R* mutation induces gene expression that has a
491 dampening effect on pMac immune responses in males.
492 ***Genes selectively upregulated in P522R females are associated with cytokine signaling and***
493 ***apoptosis***
494 As so far we have seen sex-dependent differences in pMac responses to the *P522R* mutation, we
495 did targeted transcriptomics on our female samples as well to determine which pathways might
496 be differentially implicated in the female's varied responses. Similar to our male data, when

pMacs from females are not treated with LPS, there are no significant gene expression differences between pMacs from WT females and *P522R* females (Supplemental Figure 5B).

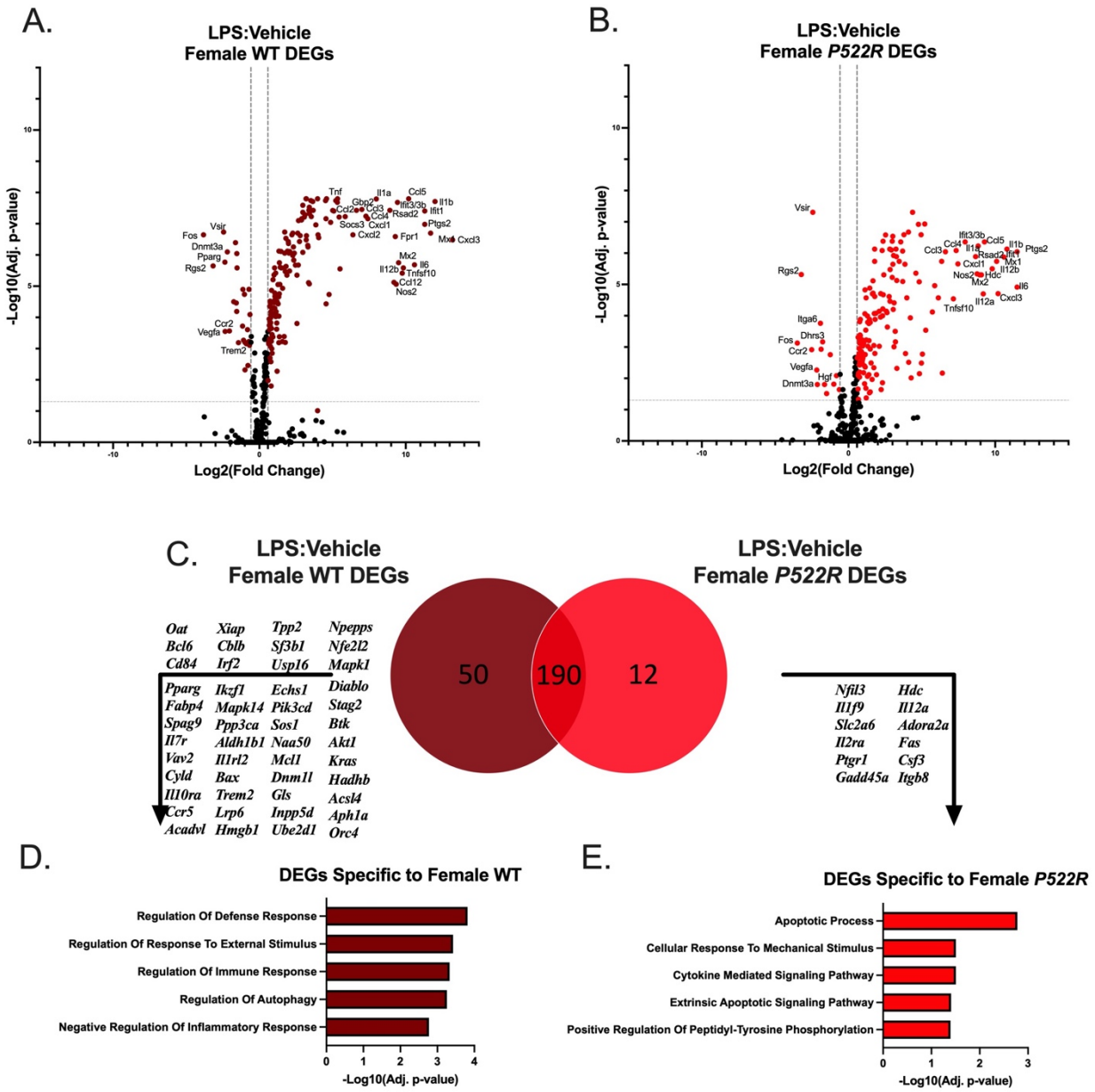

Figure 9: Genes selectively upregulated in *P522R* females are associated with cytokine signaling and apoptosis. pMacs from female WT and *P522R* mice were plated and treated with either vehicle or LPS (10ng/mL) and left to incubate for 6 hours. Cells were then collected and RNA was isolated for gene expression analysis. (A) Volcano plot comparing gene expression of LPS treated pMacs from female WT mice to gene expression of vehicle treated pMacs from female WT mice, horizontal grey dashed line indicating adjusted $p<0.05$, and vertical dashed lines indicating fold change of greater than 1.5. (B) Volcano plot comparing gene expression of LPS treated pMacs from female *P522R* mice to gene expression of vehicle treated pMacs from female *P522R* mice, horizontal grey dashed line indicating adjusted $p<0.05$, and vertical dashed lines indicating fold change of greater than 1.5. (C) Venn diagram comparing number of DEGs between pMacs from WT females and pMacs from *P522R* females after LPS

509 stimulation. (D) GO biological process pathways associated with DEGs specific to pMacs from WT females in
510 response to LPS stimulation. (D) GO biological process pathways associated with DEGs specific to pMacs from
511 *P522R* females in response to LPS stimulation.
512
513 However, upon LPS treatment, different responses to this activating stimulus occur. DEGs are
514 represented in volcano plots for pMacs from WT females after LPS treatment (Figure 9A), and
515 pMacs from *P522R* females after LPS treatment (Figure 9B). Many of the DEGs implicated in
516 the cellular response to LPS are the same between pMacs from WT and *P522R* females,
517 comprising 190 shared DEGs (Figure 9C), but each genotype did again have specific DEGs
518 related to them, with 50 DEGs specific to WT females, and 12 DEGs specific to *P522R* females
519 in response to LPS. These distinct gene groups were once again analyzed via GO biological
520 process pathway analysis, and the results were, unsurprisingly, quite distinct from the male
521 groups. We found that DEGs specific to pMacs from WT females were associated with pathways
522 including regulation of defense response, regulation of immune response, regulation of
523 autophagy, and negative regulation of the inflammatory response (Figure 9D). DEGs specific to
524 pMacs from *P522R* females on the other hand were associated with pathways including cytokine
525 mediated signaling, apoptotic processing, extrinsic apoptotic signaling, and positive regulation of
526 peptidyl-tyrosine phosphorylation (Figure 9E). This suggests that the *P522R* mutation induces
527 genes related to the upregulation of immune responses in pMacs from females.
528

529 **DISCUSSION**

530 Numerous studies have implicated the immune system as a player in the progression of
531 neurodegenerative disorders, both within the brain and in the periphery. This includes evidence
532 that peripheral monocytes and tissue-resident macrophages participate in Aβ plaque uptake, both
533 around the brain and in peripheral tissue reservoirs (22-24). Furthermore, macrophages are
534 known to be one of the main producers of inflammatory cytokines, which, when chronic, can

535 exacerbate neurodegeneration (2-4), but when acute, act as messengers to brain immune cells
536 and signals to other local immune cells (44-46). Therefore, it is of critical importance to
537 investigate the nature of peripheral immune mechanisms to identify potential new targets for
538 therapeutic intervention. With this objective in mind, many groups have studied the effects of the
539 *Plcg2-P522R* protective mutation in myeloid cells, primarily microglia, to try to determine how
540 this protection is being conferred since the effects manifest themselves in improved cognitive
541 function. However, the effect of the *P522R* mutation on peripheral tissue-resident macrophages,
542 which have become of increasing importance in the context of AD, had yet to be determined.
543 Additionally, we assessed how the mutation's effects may differ between sexes, as it is well
544 known that both AD risk and immune system function is highly affected by sex. Herein, we
545 show that the *P522R* mutation does indeed confer functional alterations in the periphery, but
546 these changes seem to vary by sex.

547 When assessing pMac sub-populations, we found that the *P522R* mutation had different
548 effects that were dependent on sex. In WT male mice, we found that our *ex vivo* cultures were
549 predominantly comprised of LPMs, making up approximately 80% of the population (the other
550 portion being made up of SPMs), and we found this to be the same in cultures obtained from
551 *P522R* males, indicating that the mutation does not have an effect on pMac sub-populations in
552 male mice. In cultures obtained from female WT mice however, we found that only around 60-
553 65% of the population on average was comprised of LPMs. The addition of the *P522R* mutation
554 altered this significantly, bringing this percentage up to closer to 80% LPMs. These data indicate
555 that the mutation alters pMac sub-populations in females but not males, and interestingly seemed
556 to bring female sub-population composition up to meet that which was found in males. Although
557 the canonical sub-populations known as LPMs and SPMs are recognized as separate groups (29),

558 recent studies have shown that not only can SPMs continue to alter their functional and
559 transcriptional profiles to look more like LPMs, and even occupy that same niche over time, but
560 they actually do so more readily in males (30, 40). It might be possible then that the *P522R*
561 mutation somehow ablates this male-bias, making it possible for the infiltrating cells to become
562 more LPM-like in females over time as is seen in males. However, it could also stand to reason
563 that this increase in LPMs in *P522R* females may happen prior to/separate from our
564 interventions, potentially during the time of peritoneum colonization by the early resident
565 macrophages. Our data is not enough from which to draw substantiated conclusions on this topic,
566 however it can be concluded that the *P522R* mutation does alter sub-populations (particularly
567 LPMs) in female mice via a currently unknown mechanism. Based on our data and the
568 aforementioned studies assessing the dynamic properties of these macrophages to shift from one
569 sub-group to another at any particular time, we decided to perform the rest of the experiments on
570 the entire population of pMacs available within a well, instead of trying to isolate LPMs and
571 SPMs specifically for functional assays. Although possible, the ability of these cells to take on
572 characteristics of the other group make this unnecessary, as these sub-populations are not static
573 regardless. We do however, use our flow data pertaining to the makeup of our populations in
574 each sex to influence our interpretation of functional results, but we do not rely solely on this for
575 the aforementioned reasons.

576 The first functions we assessed were phagocytosis and lysosomal activity, these being the
577 ability to take up particles, and the ability to break them down, respectively. The literature
578 addressing the effect of the *P522R* mutation on phagocytosis is inconsistent, showing both
579 increased and decreased phagocytosis (14-16). This discrepancy was hypothesized to be due to
580 the size of the cargo, with studies showing lower phagocytosis of larger particles such as

581 zymosan and *E. coli*, and more phagocytosis of smaller-sized dextrans (14, 15). We show here
582 that this observed difference in phagocytosis caused by the *P522R* mutation could also be due to
583 the sex in which the testing was performed. In our cultures, we found that the *P522R* mutation
584 did alter phagocytosis and lysosomal activity in pMacs, but in opposing directions in males and
585 females. Our data showed that pMacs from *P522R* males exhibited less uptake of *E. coli*
586 particles over time compared to pMacs from WT males. In females, these same differences were
587 not found, and the *P522R* mutation seemingly had little effect on *E. coli* uptake over time. We
588 further observed changes in lysosomal activity, with the *P522R* mutation significantly reducing
589 lysosomal protease activity in males, and significantly increasing it in females, further supporting
590 the sex-dependent differences this mutation confers. It should be noted however, that differences
591 in phagocytosis in males were not observed until around the 6-7 hour mark, meaning that initial
592 uptake of *E. coli* was similar between groups, but the pMacs from *P522R* males may become
593 exhausted earlier or more rapidly. Taken together, these results suggested the potential of the
594 *P522R* mutation to be positive in females, but potentially negative in males via the reduction in
595 bacterial uptake and degradation.

596 Further functional assays surveyed inflammatory cytokine secretion by pMacs from
597 females and males, as previous studies showed that the *P522R* mutation was capable of
598 increasing cytokine secretion in microglia (13). Our data indicated that this effect is also present
599 in pMacs, but to different extents in males and females. We measured cytokine release both at
600 baseline and post-LPS to determine whether there may be differences prior to any sort of
601 external stimulation. In both male and female cultures, we saw that at baseline, regardless of
602 genotype, the pMacs were not producing inflammatory cytokines, supporting that our *ex vivo*
603 culture model allows for the cells to return to baseline non-inflammatory conditions. For this

604 reason, we chose to treat the cells with the immune cell stimulant LPS to elicit an inflammatory
605 response that could be compared between the groups. After LPS stimulation, pMacs from *P522R*
606 males showed increased release of TNF, IL-6, IL-12p70, and IFN-γ over 24 hours compared to
607 pMacs from WT males, while pMacs from *P522R* females showed increased release of TNF, IL-
608 6, KC/GRO, IL-1β, IL-12p70, and IL-2 over 24 hours compared to pMacs from WT females.
609 Interestingly, the *P522R* mutation had no effect on the release of IL-10, a canonical cytokine
610 involved in the resolution of inflammatory responses, in either females or males. Although it
611 could be assumed that these increases in inflammatory cytokines could be negative, our study
612 only looked at acute cytokine secretion, which is likely to have been an adaptive and beneficial
613 response.

614 In our assays assessing the effects of the *P522R* mutation on pMac function and
615 population dynamics we found different functional outcomes depending on sex. Furthermore, we
616 found that many of these differences were more/only prominent after some form of cell
617 activation either via *E. coli* or LPS treatment. This led us to believe that the *P522R* mutation may
618 exert stronger effects upon cell activation in females and males, and we wondered whether we
619 might be able to potentially determine some cellular pathways implicated in these differential
620 responses, and therefore we performed targeted transcriptomics to assess immune cell specific
621 gene expression changes. First, we compared gene expression in pMacs from *P522R* males to
622 pMacs from WT males and found no differences at baseline. From that point, we compared gene
623 expression after LPS stimulation between these two groups to determine what changes might be
624 occurring due to the *P522R* mutation in response to cellular activation. What we found was quite
625 fascinating. We saw that in response to LPS stimulation, the DEGs specific to *P522R* males were
626 related to pathways associated with negative regulation of the immune response. This lines up

627 with the functional data that revealed that in pMacs from males, the *P522R* mutation decreases
628 phagocytosis and lysosomal activity, and does not exert as strong of an effect on inflammatory
629 cytokine secretion as is seen in females. In females however, we found that the DEGs specific to
630 pMacs from *P522R* females were quite different, being related to cytokine mediated signaling
631 pathways, positive regulation of peptidyl-tyrosine phosphorylation, and apoptotic signaling.
632 Tyrosine phosphorylation has been characterized as a main event following LPS stimulation in
633 macrophages which aids in cellular activation (47), in line with the observed increase in
634 lysosomal activity and cytokine secretion in females. Furthermore, cytokine mediated pathways
635 and apoptotic signaling can go hand in hand, as cytokines are main promoters of apoptosis,
636 particularly TNF (48, 49). It appears based on our transcriptomic data that the *P522R* mutation
637 activates different intracellular signaling pathways and concurrent gene expression in response to
638 LPS leading to the different outcomes in response to activation seen between male and females.
639 At this time, we cannot say directly how these sex-dependent responses may contribute to
640 the neuroprotection associated with this mutation. However, we can say with certainty that
641 peripheral immune cells, particularly peritoneal macrophages, are affected by the presence of this
642 mutation, and show transcriptional, lysosomal, phagocytic, and inflammatory alterations due to
643 its presence, particularly after an inflammatory challenge. With recent studies indicating a role
644 for peripheral macrophages in the progression of AD, this study opens up new avenues of
645 interest for more in-depth studies of the contribution of peripheral macrophages to the *P522R*
646 mutation's protective effects. It should be noted however, that these responses and functional
647 differences may not solely be due to intrinsic changes in macrophages due to the *P522R*
648 mutation. As we isolated these cells from the peritoneum, a location filled with many immune
649 cell types (many of which would also carry the KI *P522R* mutation), some of these functional

650 changes could be due to the macrophages' direct interaction with/response to other mutated
651 immune cells which might leave lasting impacts on macrophage function. While we hypothesize
652 that the functional changes seen in this study are due to direct intrinsic changes in macrophages
653 brought about by the *P522R* mutation, which is supported by the studies showing intrinsic
654 mechanisms of the *P522R* mutation in similar cell type microglia (12, 13), we cannot completely
655 rule out the contribution of the peritoneal environment prior to our isolation protocol.
656 Additionally, we provide ample evidence to necessitate the use of both sexes in any future study
657 aiming to assess the protective effects of this mutation. Many drugs aiming to cure or mediate
658 disease have been pulled from the market due to unforeseen issues arising in one sex or another
659 (50, 51). Over recent years the issue of sex-differences in biomedical research has come to the
660 forefront, and we provide further evidence to support the advantages of utilizing both sexes in
661 pre-clinical studies whenever possible. Although this study does not provide an exact mechanism
662 by which these peripheral macrophages may contribute to the protective effects of this mutation,
663 it provides compelling reasons to support future inquiries into these questions, which we aim to
664 do moving forward using *in vivo* models of neurodegeneration to determine whether these same
665 functional alterations directly impact neuroinflammation and cognitive performance. It further
666 supports the importance of including sex as a biological variable in studies as well, showing that
667 not only can the magnitude of response to protective genetic mutations be different between
668 sexes, but also the directionality of response can vary by sex and will have implications for
669 future therapeutic interventions.
670
671 **CONCLUSION**

672 Inflammation and the cells of the peripheral immune system have been implicated in the
673 progression of AD. Therefore, identifying pathways that could be targeted in therapeutic
674 interventions will give the field the potential to modulate these dysregulated immune cell
675 functions. Others have demonstrated that the *P522R* mutation has the ability to enhance
676 important immune functions in microglia, such as phagocytosis and cytokine secretion. Herein
677 we provide the first evidence that the *P522R* mutation also modulates peripheral tissue-resident
678 macrophage functions, and that these effects are highly sex-dependent. Taken together, these
679 results reveal that peripheral immune cell changes should be taken into account when assessing
680 the mechanism(s) by which deleterious/beneficial genetic mutations confer their effects, as
681 microglia may not be the only cells contributing to the functional outcome of the genetic variant,
682 and that sex as a biological variable should be an integral part of any study looking to assess
683 peripheral inflammatory mechanisms that are likely to affect brain function.
684
685 **LIST OF ABBREVIATIONS**
686 PLCG2, phospholipase C gamma 2
687 AD, Alzheimer's disease
688 Aβ, amyloid-beta
689 TREM2, triggering receptor expressed on myeloid cells 2
690 TLR, toll-like receptor
691 PIP2, phosphatidylinositol (4,5) bisphosphate
692 DAG, diacylglycerol
693 IP3, inositol 1,4,5 triphosphate
694 LPM, large peritoneal macrophage

695 SPM, small peritoneal macrophage

696 WT, wild-type

697 PBS, phosphate buffered saline

698 FMOC, fluorescence minus one control

699 MSD, MesoScale Discovery

700 LLOD, lower limit of detection

701 SEM, standard error of the mean

702 MHCII, major histocompatibility complex II

703 LPS, lipopolysaccharide

704 DEG, differentially expressed gene

705

706 **DECLARATIONS**

707 **Ethics approval and consent to participate**

708 Mice were utilized in accordance with protocols approved by the Institutional Animal Care and

709 Use Committee of the University of Florida.

710 **Consent for publication**

711 Not applicable.

712 **Availability of data and materials**

713 All data are included in the present study or contained within the supplemental files. Raw data

714 can be provided upon request.

715 **Competing Interests**

716 The authors declare no conflicts of interest.

717 **Funding**

The funding for this project was provided by the McKnight Brain Institute and Norman Fixel Institute for Neurological Diseases.

Authors Contributions

HAS and MGT conceived the study. HAS designed the experiments, performed them, and analyzed and interpreted the data. MLB, RLW, JJ, KBM, CC, NN, and AMT assisted with various experimental procedures. HAS designed all figures. HAS and MGT wrote and edited the manuscript. All authors approved the final version of the manuscript and figures.

Acknowledgements

The authors thank the Tansey, Khoshbouei, and Chakrabarty labs for useful discussions.

REFERENCES

1. Scheyer O, Rahman A, Hristov H, et al. Female Sex and Alzheimer's Risk: The Menopause Connection. J Prev Alzheimers Dis. 2018;5(4):225-230. doi:10.14283/jpad.2018.34
2. Cunningham C, Campion S, Lunnon K, et al. Systemic inflammation induces acute behavioral and cognitive changes and accelerates neurodegenerative disease. Biol Psychiatry. 2009;65(4):304-312. doi:10.1016/j.biopsych.2008.07.024
3. Tejera D, Mercan D, Sanchez-Caro JM, et al. Systemic inflammation impairs microglial Aβ clearance through NLRP3 inflammasome. EMBO J. 2019;38(17):e101064. doi:10.15252/embj.2018101064
4. Marshall JS, Warrington R, Watson W, Kim HL. An introduction to immunology and immunopathology. Allergy Asthma Clin Immunol. 2018;14(Suppl 2):49. Published 2018 Sep 12. doi:10.1186/s13223-018-0278-1
5. Cao W, Zheng H. Peripheral immune system in aging and Alzheimer's disease [published correction appears in Mol Neurodegener. 2018 Oct 24;13(1):58]. Mol Neurodegener. 2018;13(1):51. Published 2018 Oct 3. doi:10.1186/s13024-018-0284-2
6. van Dyck CH, Swanson CJ, Aisen P, et al. Lecanemab in Early Alzheimer's Disease. *N Engl J Med*. 2023;388(1):9-21. doi:10.1056/NEJMoa2212948
7. Kleineidam L, Chouraki V, Próchnicki T, et al. PLCG2 protective variant p.P522R modulates tau pathology and disease progression in patients with mild cognitive impairment. Acta Neuropathol. 2020;139(6):1025-1044. doi:10.1007/s00401-020-02138-6
8. Sims R, van der Lee SJ, Naj AC, et al. Rare coding variants in PLCG2, ABI3, and TREM2 implicate microglial-mediated innate immunity in Alzheimer's disease. Nat Genet. 2017;49(9):1373-1384. doi:10.1038/ng.3916

9. Jackson JT, Mulazzani E, Nutt SL, Masters SL. The role of PLCγ2 in immunological disorders, cancer, and neurodegeneration. J Biol Chem. 2021;297(2):100905. doi:10.1016/j.jbc.2021.100905
10. Magno L, Bunney TD, Mead E, Svensson F, Bictash MN. TREM2/PLCγ2 signalling in immune cells: function, structural insight, and potential therapeutic modulation. Mol Neurodegener. 2021;16(1):22. Published 2021 Apr 6. doi:10.1186/s13024-021-00436-5
11. Andreone BJ, Przybyla L, Llapashtica C, et al. Alzheimer's-associated PLCγ2 is a signaling node required for both TREM2 function and the inflammatory response in human microglia. Nat Neurosci. 2020;23(8):927-938. doi:10.1038/s41593-020-0650-6
12. Magno L, Lessard CB, Martins M, et al. Alzheimer's disease phospholipase C-gamma-2 (PLCG2) protective variant is a functional hypermorph. Alzheimers Res Ther. 2019;11(1):16. Published 2019 Feb 2. doi:10.1186/s13195-019-0469-0
13. Takalo M, Wittrahm R, Wefers B, et al. The Alzheimer's disease-associated protective Plcγ2-P522R variant promotes immune functions. Mol Neurodegener. 2020;15(1):52. Published 2020 Sep 11. doi:10.1186/s13024-020-00402-7
14. Maguire E, Menzies GE, Phillips T, et al. PIP2 depletion and altered endocytosis caused by expression of Alzheimer's disease-protective variant PLCγ2 R522. EMBO J. 2021;40(17):e105603. doi:10.15252/embj.2020105603
15. Solomon S, Sampathkumar NK, Carre I, et al. Heterozygous expression of the Alzheimer's disease-protective PLCγ2 P522R variant enhances Aβ clearance while preserving synapses. Cell Mol Life Sci. 2022;79(8):453. Published 2022 Jul 27. doi:10.1007/s00018-022-04473-1
16. Tsai AP, Dong C, Lin PB, et al. Genetic variants of phospholipase C-γ2 alter the phenotype and function of microglia and confer differential risk for Alzheimer's disease. Immunity. 2023;56(9):2121-2136.e6. doi:10.1016/j.immuni.2023.08.008
17. Gate D, Rezai-Zadeh K, Jodry D, Rentsendorj A, Town T. Macrophages in Alzheimer's disease: the blood-borne identity. J Neural Transm (Vienna). 2010;117(8):961-970. doi:10.1007/s00702-010-0422-7
18. Town T, Laouar Y, Pittenger C, et al. Blocking TGF-beta-Smad2/3 innate immune signaling mitigates Alzheimer-like pathology. Nat Med. 2008;14(6):681-687. doi:10.1038/nm1781
19. Hawkes CA, McLaurin J. Selective targeting of perivascular macrophages for clearance of beta-amyloid in cerebral amyloid angiopathy. Proc Natl Acad Sci U S A. 2009;106(4):1261-1266. doi:10.1073/pnas.0805453106
20. Malm TM, Koistinaho M, Pärepalo M, et al. Bone-marrow-derived cells contribute to the recruitment of microglial cells in response to beta-amyloid deposition in APP/PS1 double transgenic Alzheimer mice. Neurobiol Dis. 2005;18(1):134-142. doi:10.1016/j.nbd.2004.09.009
21. Simard AR, Soulet D, Gowing G, Julien JP, Rivest S. Bone marrow-derived microglia play a critical role in restricting senile plaque formation in Alzheimer's disease. Neuron. 2006;49(4):489-502. doi:10.1016/j.neuron.2006.01.022
22. Wang J, Gu BJ, Masters CL, Wang YJ. A systemic view of Alzheimer disease — insights from amyloid-β metabolism beyond the brain. Nat Rev Neurol. 2017;13(10):612-623. doi:10.1038/nrneurol.2017.111
23. Qosa H, Abuasal BS, Romero IA, et al. Differences in amyloid-β clearance across mouse and human blood–brain barrier models: Kinetic analysis and mechanistic

800 modeling. Neuropharmacology. 2014;79:668-678.
801 doi:10.1016/j.neuropharm.2014.01.023
802 24. Xiang Y, Bu XL, Liu YH, et al. Physiological amyloid-beta clearance in the periphery
803 and its therapeutic potential for Alzheimer's disease. Acta Neuropathol.
804 2015;130(4):487-499. doi:10.1007/s00401-015-1477-1
805 25. Eisele YS, Obermüller U, Heilbronner G, et al. Peripherally applied aβ-containing
806 inoculates induce cerebral β-amyloidosis. Science. 2010;330(6006):980-982.
807 doi:10.1126/science.1194516
808 26. Klein SL, Flanagan KL. Sex differences in immune responses. Nat Rev Immunol.
809 2016;16(10):626-638. doi:10.1038/nri.2016.90
810 27. Muñoz-Castro C, Mejias-Ortega M, Sanchez-Mejias E, et al. Monocyte-derived cells
811 invade brain parenchyma and amyloid plaques in human Alzheimer's disease
812 hippocampus. Acta Neuropathol Commun. 2023;11(1):31. Published 2023 Feb 28.
813 doi:10.1186/s40478-023-01530-z
814 28. Paranjpe MD, Belonwu S, Wang JK, et al. Sex-Specific Cross Tissue Meta-Analysis
815 Identifies Immune Dysregulation in Women With Alzheimer's Disease. Front Aging
816 Neurosci. 2021;13:735611. Published 2021 Sep 30. doi:10.3389/fnagi.2021.735611
817 29. Cassado Ados A, D'Império Lima MR, Bortoluci KR. Revisiting mouse peritoneal
818 macrophages: heterogeneity, development, and function. Front Immunol. 2015;6:225.
819 Published 2015 May 19. doi:10.3389/fimmu.2015.00225
820 30. Bain CC, Hawley CA, Garner H, et al. Long-lived self-renewing bone marrow-derived
821 macrophages displace embryo-derived cells to inhabit adult serous cavities. Nat
822 Commun. 2016;7:ncomms11852. Published 2016 Jun 13. doi:10.1038/ncomms11852
823 31. Zajd CM, Ziemba AM, Miralles GM, et al. Bone Marrow-Derived and elicited
824 peritoneal macrophages are not created equal: the questions asked dictate the cell type
825 used. Frontiers in Immunology. 2020;11. doi:10.3389/fimmu.2020.00269
826 32. Wang C, Yu X, Cao Q, et al. Characterization of murine macrophages from bone
827 marrow, spleen and peritoneum. BMC Immunology. 2013;14(1). doi:10.1186/1471-
828 2172-14-6
829 33. Kowalski K, Mulak A. Brain-gut-microbiota axis in alzheimer's disease. J
830 Neurogastroenterol Motil. 2019;25(1):48-60. doi:10.5056/jnm18087
831 34. Kitamura J, Nagai M, Ueno H, et al. The insular cortex, Alzheimer disease pathology,
832 and their effects on blood pressure variability. Alzheimer Disease & Associated
833 Disorders. 2020;34(3):282-291. doi:10.1097/wad.0000000000000340
834 35. Koren T, Yifa R, Amer M, et al. Insular cortex neurons encode and retrieve specific
835 immune responses. Cell. 2021;184(24):5902-5915.e17. doi:10.1016/j.cell.2021.10.013
836 36. Chen EY, Tan CM, Kou Y, et al. Enrichr: interactive and collaborative HTML5 gene list
837 enrichment analysis tool. BMC Bioinformatics. 2013;14(1):128. doi:10.1186/1471-
838 2105-14-128
839 37. Kuleshov MV, Jones MR, Rouillard AD, et al. Enrichr: a comprehensive gene set
840 enrichment analysis web server 2016 update. Nucleic Acids Res. 2016;44(W1):W90-
841 W97. doi:10.1093/nar/gkw377
842 38. Xie Z, Bailey A, Kuleshov MV, et al. Gene set knowledge discovery with enrichr.
843 Current Protocols. 2021;1(3):e90. doi:10.1002/cpz1.90

39. Ghosn EE, Cassado AA, Govoni GR, et al. Two physically, functionally, and developmentally distinct peritoneal macrophage subsets. Proc Natl Acad Sci U S A. 2010;107(6):2568-2573. doi:10.1073/pnas.0915000107
40. Bain CC, Gibson DA, Steers NJ, et al. Rate of replenishment and microenvironment contribute to the sexually dimorphic phenotype and function of peritoneal macrophages. Sci Immunol. 2020;5(48):eabc4466. doi:10.1126/sciimmunol.abc4466
41. Zhan X, Stamova B, Jin LW, DeCarli C, Phinney B, Sharp FR. Gram-negative bacterial molecules associate with Alzheimer disease pathology. Neurology. 2016;87(22):2324-2332. doi:10.1212/WNL.0000000000003391
42. Maheshwari P, Eslick GD. Bacterial infection and alzheimer's disease: a meta-analysis. JAD. 2014;43(3):957-966. doi:10.3233/JAD-140621
43. Kang YJ, Kusler B, Otsuka M, et al. Calcineurin negatively regulates tlr-mediated activation pathways. The Journal of Immunology. 2007;179(7):4598-4607. doi:10.4049/jimmunol.179.7.4598
44. Dantzer R. Neuroimmune interactions: from the brain to the immune system and vice versa. *Physiological Reviews*. 2018;98(1):477-504. doi:10.1152/physrev.00039.2016
45. Jin H, Li M, Jeong E, Castro-Martinez F, Zuker CS. A body–brain circuit that regulates body inflammatory responses. Nature. 2024;630(8017):695-703. doi:10.1038/s41586-024-07469-y
46. Zang X, Chen S, Zhu J, Ma J, Zhai Y. The emerging role of central and peripheral immune systems in neurodegenerative diseases. Front Aging Neurosci. 2022;14:872134. doi:10.3389/fnagi.2022.872134
47. Weinstein SL, Gold MR, DeFranco AL. Bacterial lipopolysaccharide stimulates protein tyrosine phosphorylation in macrophages. Proc Natl Acad Sci USA. 1991;88(10):4148-4152. doi:10.1073/pnas.88.10.4148
48. Behar SM, Martin CJ, Booty MG, et al. Apoptosis is an innate defense function of macrophages against Mycobacterium tuberculosis. Mucosal Immunology. 2011;4(3):279-287. doi:10.1038/mi.2011.3
49. Xaus J, Comalada M, Valledor AF, et al. LPS induces apoptosis in macrophages mostly through the autocrine production of TNF-α. *Blood*. 2000;95(12):3823-3831. doi:10.1182/blood.V95.12.3823
50. Soldin OP, Mattison DR. Sex differences in pharmacokinetics and pharmacodynamics: Clinical Pharmacokinetics. 2009;48(3):143-157. doi:10.2165/00003088-200948030-00001
51. U.S. Government Accountability Office. *Drug Safety: Most Drugs Withdrawn in Recent Years Had Greater Health Risks for Women.* 2001. GAO-01-286R. Accessed August 22, 2024.